King Saud University

Journal of Saudi Chemical Society

www.ksu.edu.sa
www.sciencedirect.com

CrossMark

Conventional and microwave synthesis, spectral, thermal and antimicrobial studies of some transition metal complexes containing 2-amino-5-methylthiazole moiety

A.P. Mishra, Rajendra K. Jain *

Department of Chemistry, Synthetic Inorganic & Coordination Chemistry Laboratories, Dr. H.S. Gour Central University, Sagar, M.P. 470 003, India

Abstract Schiff base metal complexes of Cr(III), Co(II), Ni(II) and Cu(II) derived from 5-chloro-salicylidene-2-amino-5-methylthiazole (HL[1]) and 2-hydroxy-1-naphthylidene-2-amino-5-methylthiazole (HL[2]) have been synthesized by conventional as well as microwave methods. These compounds have been characterized by elemental analysis, FT-IR, FAB-mass, molar conductance, electronic spectra, ^{1}H-NMR, ESR, magnetic susceptibility, thermal, electrical conductivity and XRD analyses. The complexes exhibit coordination number 4 or 6. The complexes are coloured and stable in air. Analytical data reveal that all the complexes exhibit 1:2 (metal:ligand) ratio. IR data show that the ligand coordinates with the metal ions in a bidentate manner through the phenolic oxygen and azomethine nitrogen. FAB-mass and thermal data show degradation pattern of the complexes. The thermal behaviour of metal complexes shows that the hydrated complexes lose water molecules of hydration in the first step; followed by decomposition of ligand molecules in the subsequent steps. XRD patterns indicate crystalline nature for the complexes. The Schiff bases and metal complexes show good activity against the Gram-positive bacteria; *Staphylococcus aureus* and Gram-negative bacteria; *Escherichia coli* and fungi *Aspergillus niger* and *Candida albicans*. The antimicrobial results also indicate that the metal complexes are better antimicrobial agents as compared to the Schiff bases.

* Corresponding author. Mob. No.: +91 9981857386.
E-mail addresses: apm19@rediffmail.com (A.P. Mishra), jainraj-chem@gmail.com (R.K. Jain).
Peer review under responsibility of King Saud University.

ELSEVIER **Production and hosting by Elsevier**

1. Introduction

Schiff base ligands have been widely studied in the field of coordination chemistry mainly due to their facile syntheses, easy availability, electronic properties and good solubility in common solvents. Transition metal complexes containing the Schiff base ligands have been of interest for many years because the transition metal complexes play a central role in the conduction of molecular materials, which display unusual conducting, magnetic, thermal properties and find applicability in material chemistry and biochemistry (Chandra et al., 2009; Chandra and Kumar, 2005). A large number of Schiff bases and their metal complexes have been found to possess important biological and catalytic activity. Due to their great flexibility and diverse structural aspects, a wide range of Schiff bases have been synthesized and their complexation behaviour was studied (Soliman and Mohamed, 2004). Heterocyclic compounds are very widely distributed in nature and are essential to many fields of material science and biological systems. Metal complexes with these ligands are becoming increasingly important as biochemical, analytical and antimicrobial reagents in the design of molecular magnets, material chemistry and so on. Various heterocycles, especially thiazole and pyridine, occupy an important place owing to their versatile activities due to the presence of multifunctional groups. Thiazole and its derivatives play a significant part in industry and biology (Spinu et al., 2001). Benzothiazoles are used for the production of dyes with photosensitizing properties (Issa et al., 2008; Chohan, 1999).

Microwave-assisted synthesis is a branch of green chemistry. The application of microwave-assisted synthesis in organic, organometallic and coordination chemistry continues to develop at an astonishing pace. Microwave-irradiated reactions under solvent free or less solvent conditions are attractive offering reduced pollution, low cost and offer high yields together with simplicity in processing and handling. The salient features of microwave approach are shorter reaction times, simple reaction conditions and enhancements in yields. (Mahajan et al., 2007, 2009; Mohanan et al., 2008; Garg et al., 2006; Sharma et al., 2010; Sun et al., 2010) Reports on the synthesis of metal complexes by microwave methods have been comparatively less.

In the present paper, we have described the coordination behaviour of novel Schiff bases (Fig. 1) derived from the condensation of 5-chlorosalicylaldehyde with 2-amino-5-methylthiazole (HL^1) and 2-hdroxy-1-naphthaldehyde with 2-amino-5-methylthiazole (HL^2) towards some transition elements, which may help in more understanding of the mode of chelation of ligands towards metals. For this purpose the complexes of Cr(III), Co(II), Ni(II) and Cu(II) ions (Figs. 2 and 3) with HL^1 and HL^2 have been synthesized by both conventional as well as microwave methods and characterized by the various physicochemical and spectral analyses. These ligands coordinate with metal ions in a bidentate manner through the phenolic oxygen and azomethine nitrogen. The metal complexes formed with these two new ligands may be used as precursors for the synthesis of new compounds. Some of which may exhibit interesting physical and chemical properties and potentially useful biological activities.

2. Experiment

2.1. Materials and instrumentation

All the chemicals and solvents used were of Anal R grade. All the reagents used for the preparation of the Schiff bases were obtained from Sigma Aldrich. Metal salts were purchased from Loba Chemie. Elemental analyses were performed on an Elementar Vario EL III Carlo Erba 1108 analyzer. FAB-mass spectra were recorded on a JEOL SX 102/DA 6000 Mass Spectrometer using argon/xenon (6 kV, 10 mA) as the FAB gas. The accelerating voltage was 10 kV and the spectra were recorded at room temperature. Electronic spectra (in DMSO) were recorded on Perkin Elmer Lambda-2B-spectrophotometer. Molar conductance measurements were conducted using 10^{-3} M solutions of the complexes in DMSO on Elico-CM 82 Conductivity Bridge at room temperature. Magnetic susceptibility measurements were carried out on a Gouy balance at room temperature using Hg[Co(SCN)$_4$] as the calibrant. Diamagnetic corrections were applied in compliance with Pascal's constant. FT-IR spectra were recorded in KBr pellets on a Perkin Elmer RX1 spectrophotometer in wave number region 4000–400 cm^{-1}. ^{1}H-NMR spectra were recorded on a JEOL AL300 FTNMR spectrometer employing TMS as internal reference and DMSO-d$_6$ as solvent. X-band EPR spectra were recorded on a Varian E-112 spectrometer at room temperature operating at the X-band region with 100 kHz modulation frequency, 5 microwave power and 1 G modulation amplitude using TCNE as the internal standard. Thermogravimetric analysis was carried out under atmospheric condition with a heating rate 10 °C min^{-1} on TGA Q500 universal V4.5A TA instrument. Powder X-ray diffraction (XRD) patterns were recorded on a RINT2000 wide angle goniometer. X-ray diffractometer, operated at 40 kV and 30 mA generator using the CuKα line at 1.54056 Å as the radiation sources. Sample was scanned between 5° and 70° (2θ) at 25 °C. The solid state electrical conductivity has been measured by impedance spectroscopic method using HIOKI 3532-50 LCR Hitester at fixed frequency 1 kHz in the temperature range of 298–413 K. Microwave-assisted synthesis were carried out in open glass vessel on a modified microwave oven model 2001 ETB
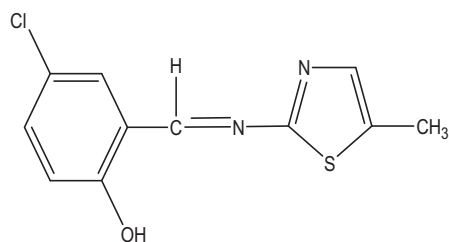
5-chlorosalicylidene-2-amino-5-methylthiazole (HL^1)
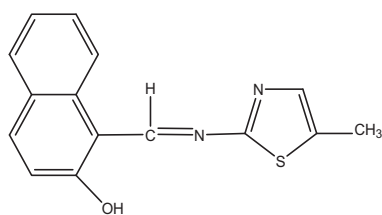
2-hydroxy-1-naphthylidene-2-amino-5-methylthiazole (HL^2)

Figure 1   Structure of the Schiff base ligands.
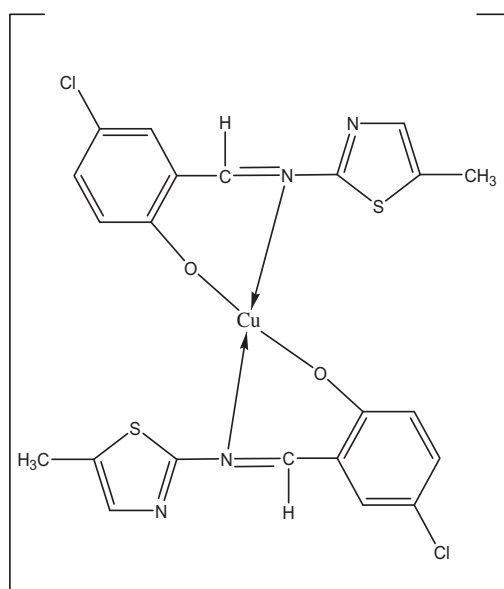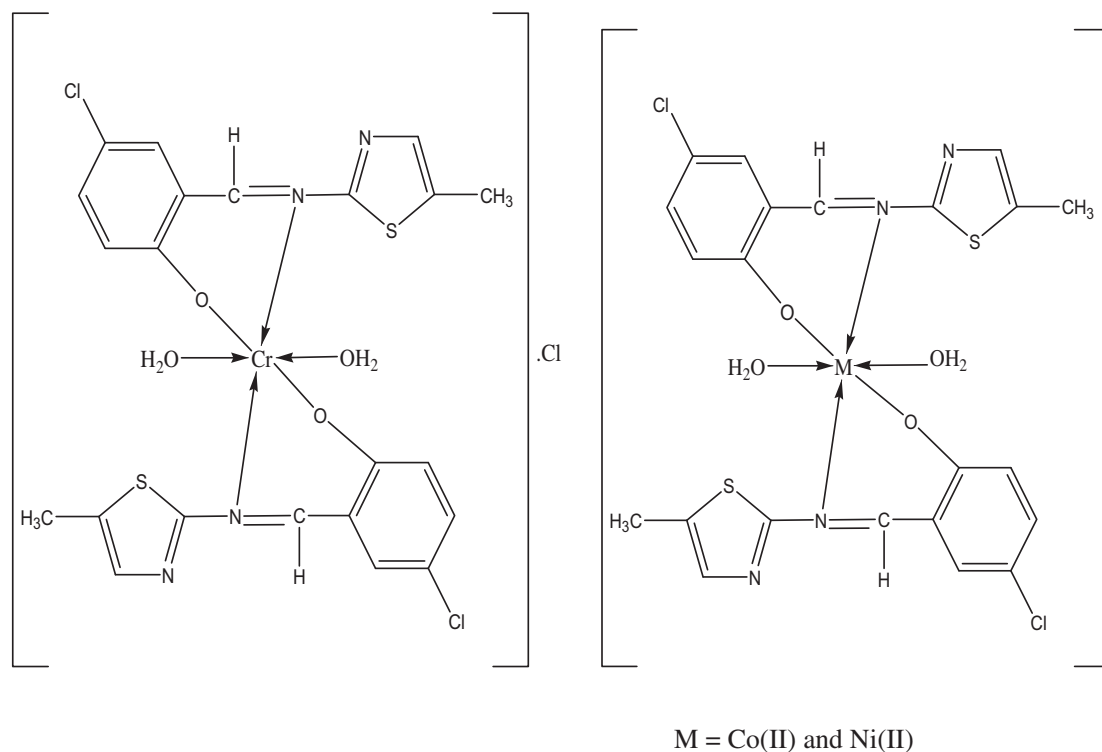
M = Co(II) and Ni(II)

Figure 2 Proposed structures of metal complexes of HL[1].

with a rotating tray and a power source 230 V, microwave energy output 800 W and microwave frequency 2450 MHz. A thermocouple device was used to monitor the temperature inside the vessel of the microwave. The microwave reactions were performed using ON/OFF cycling to control the temperature.

2.2. Biological activity

The *in vitro* biological activity of the Schiff bases and their complexes was tested against the bacteria *Escherichia coli*

and *Staphylococcus aureus* by disc diffusion method using nutrient agar as the medium and streptomycin as the control. The antifungal activities of the compounds were also tested by the Well diffusion method against the fungi *Aspergillus niger* and *Candida albicans*, on potato dextrose agar as the medium and miconazole as the control. Each of the compounds was dissolved in DMSO and the solutions of the concentrations (25, 50 and 100 ppm) were prepared separately. In a typical procedure, a well was made on the agar medium inoculated with microorganism. The well was filled with the test solution using a micropipette and the plate was incubated 24 h for bacteria at 37 °C and 72 h for fungi at 30 °C. During this period,

M = Co(II) and Ni(II)
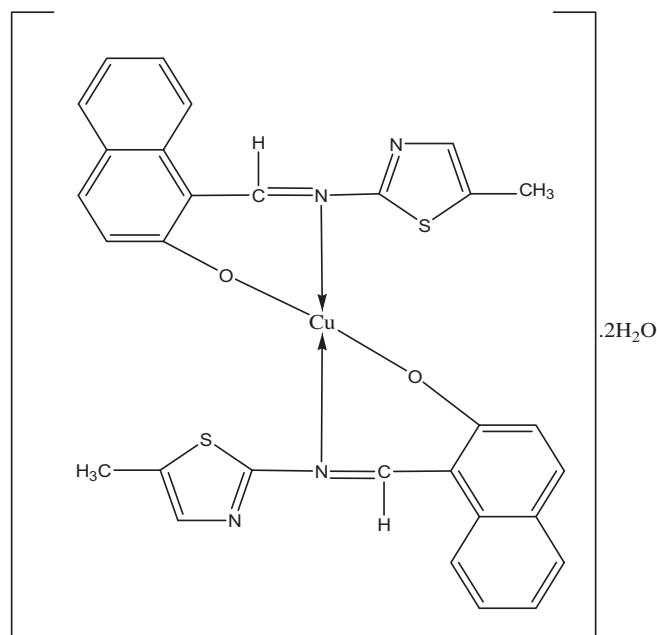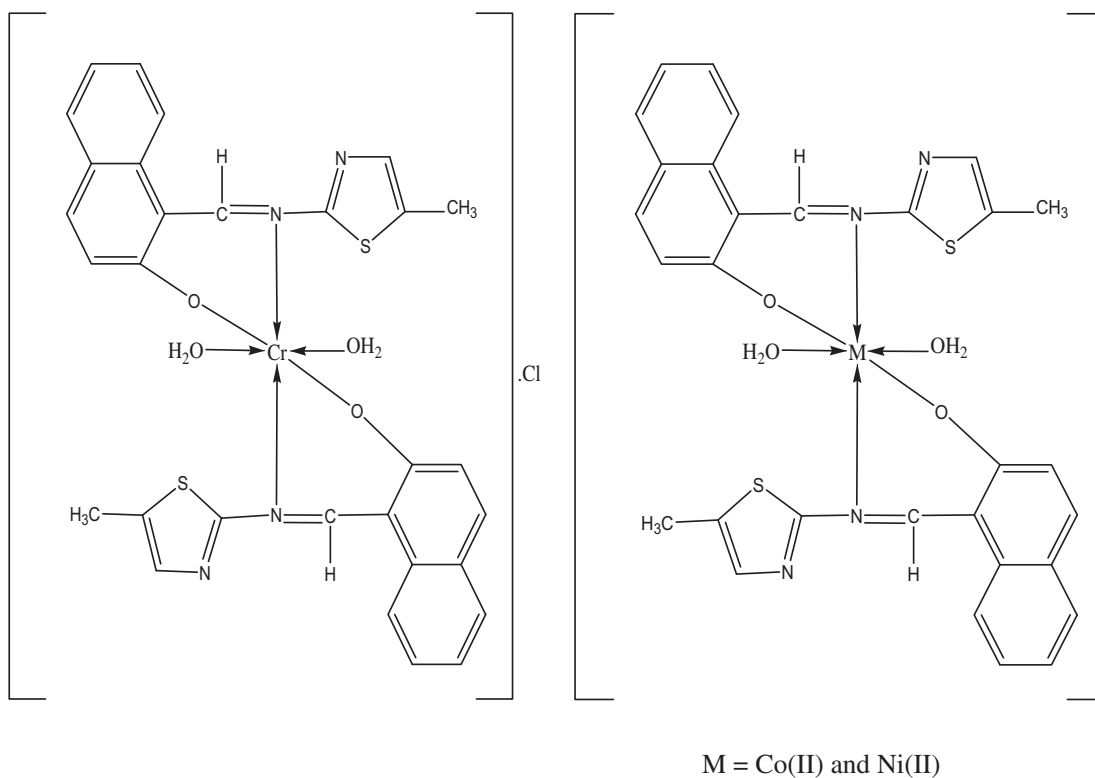
Figure 3 Proposed structures of metal complexes of HL^2.

the test solution diffused and the growth of the inoculated microorganism was affected. The inhibition zone was developed, at which the concentration was noted.

2.3. Conventional method for the synthesis of Schiff bases

HL^1 and HL^2 Schiff bases were synthesized by the condensation of an equimolar ratio of 5-chlorosalicylaldehyde and 2-

hydroxy-1-naphthaldehyde with 2-amino-5-methylthiazole dissolved in ethanol. The resulting reaction mixture was stirred well, refluxed for 3–4 h and then allowed to cool overnight. The coloured solid precipitate of Schiff base obtained was filtered, washed with cold ethanol several times and dried in air at room temperature and finally stored under reduced pressure in a CaCl$_2$ desiccator. The purity of the synthesized compounds was checked by TLC using silica gel G (yield: 77–80%).

2.4. Microwave method for the synthesis of Schiff bases

The equimolar (1:1) ratio of 5-bromosalicylaldehyde and 2-hydroxy-1-naphthaldehyde with 2-amino-5-nitrothiazole was mixed thoroughly in a grinder. The reaction mixture was then irradiated by the microwave oven by taking 3–4 mL of dry ethanol as a solvent. The reaction was completed in a short time (4–5 min) with higher yields. The resulting product was then recrystallized with ethanol, finally dried under reduced pressure over anhydrous $CaCl_2$ in a desiccator. The progress of the reaction, purity of the product was monitored by TLC using silica gel G (yield: 88–90%).

2.5. Conventional method for the synthesis of metal complexes

The metal complexes were prepared by the mixing of (50 mL) ethanolic solution of $CrCl_3 \cdot 6H_2O/CoCl_2 \cdot 6H_2O/NiCl_2 \cdot 6H_2O/CuCl_2 \cdot 2H_2O$ with the (50 mL) ethanolic solution of Schiff bases (HL^1/HL^2) in a 1:2 (metal:ligand) ratio. The resulting mixture was refluxed on water bath for 5–9 h. A coloured product appeared on standing and cooling the above solution. The precipitated complex was filtered, washed with ether and recrystallized with ethanol several times and dried under the reduced pressure over anhydrous $CaCl_2$ in a desiccator. It was further dried in an electric oven at 50–70 °C (yield: 58–74%).

2.6. Microwave method for the synthesis of metal complexes

The ligand and the metal salts were mixed in a 1:2 (metal:ligand) ratio in a grinder. The reaction mixture was then irradiated by the microwave oven by taking 3–4 mL of dry ethanol as a solvent. The reaction was completed in a short time (6–10 min) with higher yields. The resulting product was then recrystallized with ethanol and ether and finally dried under reduced pressure over anhydrous $CaCl_2$ in a desiccator. The progress of the reaction and purity of the product was monitored by TLC using silica gel G (yield: 75–86%).

3. Results and discussion

As a result of the microwave-assisted synthesis, it was observed that the reaction was completed in a short time with higher yields compared to the conventional method. In the microwave method homogeneity of the reaction mixture was increased by the rotation of the reaction platform tray. The confirmation of the results was also checked by repeating the synthesis process. Comparative study results obtained by microwave-assisted synthesis; versus conventional heating method is that some reactions which required 3.1–8.6 h by conventional method, were completed within 4.2–8.9 min by the microwave irradiation technique, yields have been improved from 58–80% to 81–90%.

All the metal complexes are coloured, solid and stable towards air and moisture at room temperature. They decompose on heating at high temperature, more or less soluble in common organic solvents. Analytical data of the compounds and together with their proposed molecular formula are given in Table 1. All the metal chelates have 1:2 (metal:ligand) stoichiometry. The observed molar conductance of the complexes

Table 1 Analytical and physical data of the compounds.

Compound (colour)	Elemental analysis, found (calcd.)%			
	C	H	N	M
HL^1 (Yellow)	51.8 (52.3)	3.2 (3.6)	10.8 (11.1)	–
$[Cr(L^1)_2(H_2O)_2].Cl$ (Yellowish brown)	41.6 (42.2)	2.6 (3.2)	8.7 (8.9)	8.1 (8.3)
$[Co(L^1)_2(H_2O)_2]$ (Purple)	42.9 (44.2)	3.2 (3.4)	9.1 (9.4)	9.1 (9.9)
$[Ni(L^1)_2(H_2O)_2]$ (Brown)	44.1 (44.2)	3.4 (3.4)	8.9 (9.4)	9.6 (9.8)
$[Cu(L^1)_2]$ (Coffee brown)	45.8 (46.6)	2.3 (2.8)	9.4 (9.9)	11.2 (11.2)
HL^2 (Light brown)	66.5 (67.1)	4.2 (4.3)	10.2 (10.4)	–
$[Cr(L^2)_2(H_2O)_2].Cl$ (Greenish brown)	54.6 (54.8)	3.6 (4.0)	8.0 (8.5)	7.1 (7.9)
$[Co(L^2)_2(H_2O)_2]$ (Dark brown)	57.0 (57.2)	4.0 (4.2)	8.7 (8.9)	8.4 (8.9)
$[Ni(L^2)_2(H_2O)_2]$ (Greenish yellow)	55.2 (57.3)	4.1 (4.2)	8.2 (8.9)	8.5 (8.9)
$[Cu(L^2)_2].2H_2O$ (Reddish brown)	56.2 (56.8)	4 (4.1)	8.3 (8.8)	9.5 (10.0)

in DMSO at room temperature are consistent with the non-electrolytic nature of the complexes except Cr(III) complex of both the Schiff base ligands, which was electrolytic in nature. The comparative results of conventional and microwave methods, molar conductance and magnetic moment data are given in Table 2.

3.1. FAB-mass spectrum

The FAB-mass spectra suggested that all the complexes have a monomeric nature. These complexes show molecular ion peaks in good agreement with the empirical formula suggested by elemental analyses.

The FAB-mass spectrum of the $[Co(L^1)_2(H_2O)_2]$ complex shows a characteristic molecular ion (M^+) peak at $m/z = 599$, which corresponds to the molecular weight of the complex for a monomeric structure. The mass spectrum shows multiple peaks representing successive degradation of the complex molecule by the formation of different fragments. The peaks of appreciable intensity have been observed at m/z values, obs.(calcd.) – 599(598), 560(562), 535(532), 467(461), 290(295), 117(119) suggesting the fragmentation pattern. The m/z value 599 corresponds to the nearest composition of $[Co(L^1)_2(H_2O)_2]$ and 117 corresponds to Co metal with chelated O, N ligand moiety.

The FAB-mass of the $[Cr(L^2)_2(H_2O)_2]Cl$ complex exhibited the molecular ion (M^+) peak at $m/z = 660$ suggesting the monomeric nature of the complex. The other important peaks of appreciable intensity have been observed at the m/z values, obs.(calcd.) – 620(623), 582(587), 560(557), 391(391), 107(113) suggesting the ion species after the successive fragmentation of different groups. The intensities of these peaks give the idea of the stabilities of the fragments. The m/z value 660 corresponds to the nearest composition $[Cr(L^2)_2(H_2O)_2] \cdot Cl$ and 107 to Cr metal with chelated N, O ligand moiety (Dubey et al., 2008; Mishra and Soni, 2008).

Table 2 Comparative results of conventional and microwave methods, molar conductance and magnetic moment data of the compounds.

Compound	Reaction period		Yield (%)		Λ_m ($\Omega^{-1}cm^2mol^{-1}$)	μ_{eff} (B.M.)
	CM (h)	MM (min)	CM	MM		
HL^1	3.1	4.2	80	90	–	–
[Cr(L^1)$_2$(H$_2$O)$_2$]·Cl	8.0	8.2	58	80	86.2	3.91
[Co(L^1)$_2$(H$_2$O)$_2$]	7.3	6.9	67	85	15.6	5.10
[Ni(L^1)$_2$(H$_2$O)$_2$]	6.5	7.0	65	83	11.9	3.09
[Cu(L^1)$_2$]	6.1	7.1	74	86	9.5	1.98
HL^2	3.9	5.1	76	(88)	–	–
[Cr(L^2)$_2$(H$_2$O)$_2$]·Cl	8.6	8.9	61	75	80.2	3.94
[Co(L^2)$_2$(H$_2$O)$_2$]	7.0	7.8	68	82	16.5	5.12
[Ni(L^2)$_2$(H$_2$O)$_2$]	6.8	8.1	63	80	11.4	3.12
[Cu(L^2)$_2$]·2H$_2$O	7.6	7.2	71	81	8.6	2.02

CM = Conventional method; MM = Microwave method.

3.2. ^{1}H-NMR spectra

The proton NMR spectra of the Schiff base ligands were recorded in DMSO-d$_6$ solution using TMS as internal standard. The ^{1}H-NMR spectra of the HL^1 and HL^2 ligands show multiplet at δ 7.405–7.765 and 7.345–7.709 ppm due to aromatic protons, singlet at δ 6.926 and 7.105 ppm for thiazole proton, singlet at δ 2.512 and 2.590 ppm for methyl proton, whilst the azomethine proton resonates as singlet at δ 8.906 and 8.985 ppm. The phenolic and naptholic OH groups have signals at δ 12.312 and 12.468 ppm which disappeared on deuteration (Ourari et al., 2006; Raman et al., 2007).

3.3. IR spectra

The data of the IR spectra of Schiff base ligands and their complexes are listed in Table 3. The IR spectra of the complexes were compared with those of the free ligand in order to determine the involvement of the coordination sites in chelation. Characteristic peaks in the spectra of the ligand and complexes were considered and compared.

IR spectrum of the HL^1 ligand exhibit the most characteristic bands at 3298 cm^{-1} v(O–H), 1628 cm^{-1} v(C = N, azomethine), 1536 cm^{-1} v(C = N, thiazole), 1244 cm^{-1} v(C–O) and 727 cm^{-1} v(C–S–C). The metal complexes of Cr(III), Co(II) and Ni(II) show a broad band at 3362–3381 cm^{-1} which may be due to v$_{str}$(OH). A medium intensity band at 813, 808 and 815 cm^{-1} in Cr(III), Co(II) and Ni(II), respectively, suggests the presence of coordinated water in these complexes.

But these bands are not observed in Cu(II) complex indicating the absence of water molecules in the Cu(II) complex. The band 1628 cm^{-1} due to the azomethine group of the Schiff base has shifted to lower frequency (1596–1608 cm^{-1}) after complexation, indicating the bonding of nitrogen of the azomethine group to the metal ion, this can be explained by the donation of electrons from nitrogen to the empty d-orbital of the metal atom. The phenolic C–O stretching vibration that appeared at 1244 cm^{-1} in Schiff base shift towards higher frequencies (27–35 cm^{-1}) in the complexes. This shift confirms the participation of oxygen in the C–O–M bond. In the IR spectra of the complexes, the stretching vibration of the free ligand v(O–H) 3298 cm^{-1} is not observed, suggesting deprotonation of the hydroxyl group and formation of M–O bonds. In the low frequency region, the band of weak intensity observed for the complexes in the region 524–544 cm^{-1} is attributed to (M–O), in the region 489–494 cm^{-1} to (M–N). The v(C = N) at 1536 cm^{-1} and v(C–S–C) at 727 cm^{-1} of the thiazole ring remain unchanged suggesting that the thiazole group does not coordinate to metal ion by neither nitrogen nor sulphur atom (Nakamoto, 1998; Omar and Mohamed, 2005; Mishra et al., 2009; Abdallah et al., 2010; Neelakantan et al., 2008).

IR spectrum of the HL^2 ligand show the most characteristic bands at 3308 cm^{-1} v(O–H), 1631 cm^{-1} v(C = N, azomethine), 1548 cm^{-1} v(C = N, thiazole), 1251 cm^{-1} v(C–O) and 738 cm^{-1} v(C–S–C). All the metal complexes show a broad band at (3378–3410 cm^{-1}) which may be due to v$_{str}$(OH). A medium intensity band at 812, 817 and 819 cm^{-1} in Cr(III), Co(II) and Ni(II), respectively, suggests the presence of coordi-

Table 3 IR bands of Schiff base ligands and their complexes.

Compound	v(C = N)	v(O–H)	v(C–O)	v(C–S–C)	v(C = N thiazole ring)	v(H$_2$O)	v(M–O)	v(M–N)
HL^1	1628	3298	1244	727	1536	–	–	–
[Cr(L^1)$_2$(H$_2$O)$_2$]·Cl	1604	–	1271	728	1538	3362, 813	532	490
[Co(L^1)$_2$(H$_2$O)$_2$]	1608	–	1279	730	1541	3381, 808	524	489
[Ni(L^1)$_2$(H$_2$O)$_2$]	1602	–	1272	729	1540	3378, 815	530	494
[Cu(L^1)$_2$]	1596	–	1275	731	1537	–	544	491
HL^2	1631	3308	1251	738	1548	–	–	–
[Cr(L^2)$_2$(H$_2$O)$_2$]·Cl	1602	–	1286	739	1550	3386, 812	546	496
[Co(L^2)$_2$(H$_2$O)$_2$]	1599	–	1281	738	1552	3378, 817	540	501
[Ni(L^2)$_2$(H$_2$O)$_2$]	1607	–	1285	740	1549	3392, 819	542	489
[Cu(L^2)$_2$]·2H$_2$O	1604	–	1290	742	1551	3410	537	499

nated water molecules in these complexes. But this band is not observed in the Cu(II) complex indicating the absence of coordinated water molecules in the Cu(II) complex. The band $1631\ cm^{-1}$ due to the azomethine group of the Schiff base has shifted to lower frequency ($1599–1607\ cm^{-1}$) after complexation. This indicates the involvement of azomethine nitrogen to the metal ion. The phenolic C–O stretching vibration that appeared at $1251\ cm^{-1}$ in Schiff base shifts towards higher frequencies ($30–39\ cm^{-1}$) in the complexes. This shift confirms the participation of oxygen in the C–O–M bond. In the IR spectra of the complexes, the stretching vibration of the free ligand ν(O–H) $3308\ cm^{-1}$ is not observed, suggesting the deprotonation of the hydroxyl group and the formation of M-O bond. In the low frequency region, the band of weak intensity observed for the complexes in the region $537–546\ cm^{-1}$ is attributed to (M–O), in the region $489–501\ cm^{-1}$ to (M–N). The ν(C = N) at $1548\ cm^{-1}$ and ν(C–S–C) at $738\ cm^{-1}$ of the thiazole ring remain unchanged suggesting that the thiazole group does not participate in coordination to the metal ion (Nakamoto, 1998; Omar and Mohamed, 2005; Mishra et al., 2009; Abdallah et al., 2010; Neelakantan et al., 2008).

The IR data of both the Schiff base and its metal complexes show that the Schiff bases (HL^1 and HL^2) are coordinated to the metal ion in bidentate manner with ON donor sites of the deprotonated phenolic oxygen and azomethine nitrogen.

3.4. Electronic spectra and magnetic moment

The electronic spectral data of the metal complexes in DMSO solution are given in Table 4. The nature of the ligand field

around the metal ion has been deduced from the electronic spectra.

The electronic spectra of Cr(III) complex of HL^1 observed bands in the region 18,205, 24,650 and 35,450 cm^{-1}, which may be assigned to $^4A_{2g}{\rightarrow}^4T_{2g}$(F) ($\nu_1$), $^4A_{2g}{\rightarrow}^4T_{1g}$(F) ($\nu_2$) and $^4A_{2g}{\rightarrow}^4T_{1g}$(P) ($\nu_3$) transitions, respectively. The magnetic moment is 3.91 B.M. Thus the octahedral geometry has been suggested for this complex. The electronic spectrum of Co(II) complex of HL^1 exhibits three bands in the range of 9344, 15,352 and 20,328 cm^{-1} which have been tentatively assigned to $^4T_{1g}{\rightarrow}^4T_{2g}$(F) ($\nu_1$), $^4T_{1g}{\rightarrow}^4A_{2g}$(F) ($\nu_2$) and $^4T_{1g}{\rightarrow}^4T_{1g}$(P) ($\nu_3$) transitions, respectively. The value of magnetic moment is 5.09 B.M.; which indicates the presence of Co(II) complex in octahedral geometry. The absorption spectrum of Ni(II) complex of HL^1 displayed three bands at 10,568, 18,846 and 23,954 cm^{-1}, which have been tentatively assigned to the transitions $^3A_{2g}{\rightarrow}^3T_{2g}$ (F)(ν_1), $^3A_{2g}{\rightarrow}^3T_{1g}$ (F) (ν_2) and $^3A_{2g}{\rightarrow}^3T_{1g}$ (P) (ν_3) respectively. The value of magnetic moment is 3.11 B.M.; therefore the octahedral geometry has been suggested for this complex. The electronic spectrum of the Cu(II) complex of HL^1 shows two bands at 13,388 and 17,660 cm^{-1} assignable to $^2B_{1g}{\rightarrow}^2B_{2g}$ and $^2B_{1g}{\rightarrow}^2E_g$ transitions, respectively. Since the value of the magnetic moment is found 1.98 B.M.; therefore square planar geometry has been suggested for Cu(II) complex.

The Cr(III) complex of HL^2 shows electronic spectral bands at 17,930, 24,691 and 35872 cm^{-1} these are tentatively assigned to $^4A_{2g}{\rightarrow}^4T_{2g}$(F) ($\nu_1$), $^4A_{2g}{\rightarrow}^4T_1$(F) ($\nu_2$) and $^4A_{2g}{\rightarrow}^4T_{1g}$(P) ($\nu_3$) transitions, respectively. The magnetic moment value is 3.94 B.M. Thus the octahedral structure has been suggested for this complex. The electronic spectrum of Co(II) complex

Table 4 Electronic spectral data and ligand field parameters of complexes.

Complex	Spectral bands (cm^{-1})	Transitions	Ligand field parameter				
			10 Dq (cm^{-1})	B (cm^{-1})	β	$\beta\%$	LFSE (kJ mol^{-1})
[Cr(L^1)$_2$(H$_2$O)$_2$]·Cl	18,205	$^4A_{2g}{\rightarrow}^4T_{2g}$(F) ($\nu_1$)	18,205	622.35	0.60	39.58	261.04
	24,650	$^4A_{2g}{\rightarrow}^4T_{1g}$(F) ($\nu_2$)					
	35,450	$^4A_{2g}{\rightarrow}^4T_{1g}$(P) ($\nu_3$)					
[Co(L^1)$_2$(H$_2$O)$_2$]	9344	$^4T_{1g}{\rightarrow}^4T_{2g}$(F) ($\nu_1$)	10,545	811.17	0.72	27.57	100.79
	15,352	$^4T_{1g}{\rightarrow}^4A_{2g}$(F) ($\nu_2$)					
	20,328	$^4T_{1g}{\rightarrow}^4T_{1g}$(P) ($\nu_3$)					
[Ni(L^1)$_2$(H$_2$O)$_2$]	10,568	$^3A_{2g}{\rightarrow}^3T_{2g}$(F) ($\nu_1$)	10,568	739.73	0.71	28.94	151.51
	18,846	$^3A_{2g}{\rightarrow}^3T_{1g}$(F) ($\nu_2$)					
	23,954	$^3A_{2g}{\rightarrow}^3T_{1g}$(P) ($\nu_3$)					
[Cu(L^1)$_2$]	13,388	$^2B_{1g}{\rightarrow}^2B_{2g}$	–	–	–	–	–
	17,660	$^2B_{1g}{\rightarrow}^2E_g$					
[Cr(L^2)$_2$(H$_2$O)$_2$]·Cl	17,930	$^4A_{2g}{\rightarrow}^4T_{2g}$(F) ($\nu_1$)	17,930	664.07	0.64	35.53	257.06
	24,691	$^4A_{2g}{\rightarrow}^4T_{1g}$(F) ($\nu_2$)					
	35,872	$^4A_{2g}{\rightarrow}^4T_{1g}$(P) ($\nu_3$)					
[Co(L^2)$_2$(H$_2$O)$_2$]	9505	$^4T_{1g}{\rightarrow}^4T_{2g}$(F) ($\nu_1$)	10,681	762.93	0.68	31.88	102.09
	15,680	$^4T_{1g}{\rightarrow}^4A_{2g}$(F) ($\nu_2$)					
	19,792	$^4T_{1g}{\rightarrow}^4T_{1g}$(P) ($\nu_3$)					
[Ni(L^2)$_2$(H$_2$O)$_2$]	11,120	$^3A_{2g}{\rightarrow}^3T_{2g}$(F) ($\nu_1$)	11,120	614.20	0.59	40.10	159.43
	18,677	$^3A_{2g}{\rightarrow}^3T_{1g}$(F) ($\nu_2$)					
	23,896	$^3A_{2g}{\rightarrow}^3T_{1g}$(P) ($\nu_3$)					
[Cu(L^2)$_2$]·2H$_2$O	13,982	$^2B_{1g}{\rightarrow}^2B_{2g}$	–	–	–	–	–
	19,112	$^2B_{1g}{\rightarrow}^2E_g$					

of HL^2 exhibits three bands at 9505, 15,680 and 19,792, these are tentatively assigned to $^4T_{1g} \rightarrow {}^4T_{2g}(F)$ (ν_1), $^4T_{1g} \rightarrow {}^4A_{2g}(F)$ (ν_2) and $^4T_{1g} \rightarrow {}^4T_{1g}(P)$ (ν_3) transitions, respectively. The magnetic moment value is 5.12 B.M.; which is indicative of octahedral geometry. The electronic spectrum of the Ni(II) complex of HL^2 shows three bands at 11,120, 18,677 and 23,896 cm^{-1} assignable to $^3A_{2g} \rightarrow {}^3T_{2g}$ (F)(ν_1), $^3A_{2g} \rightarrow {}^3T_{1g}$ (F)(ν_2) and $^3A_{2g} \rightarrow {}^3T_{1g}(P)$ (ν_3) transitions, respectively. The value of the magnetic moment is 3.12 B.M.; therefore octahedral geometry has been suggested for this complex. The electronic spectrum of the Cu(II) complex of HL^2 shows two bands at 13,982 and 19,112 cm^{-1} assignable to $^2B_{1g} \rightarrow {}^2B_{2g}$ and $^2B_{1g} \rightarrow {}^2E_g$ transitions, respectively. The value of magnetic moment for this complex is 2.02 B.M.; thus the square planar geometry has been suggested for Cu(II) complex.

The different parameters such as ligand field splitting energy (10 Dq), Racah inter-electronic repulsion parameter (B), nephelauxetic ratio (β), percent of covalent character (β%) and ligand field stabilization energy (LFSE) have been calculated, the values of these parameters are given in Table 4. The complexes show the lower value of B than that of the free ion which indicates the orbital overlapping, delocalization of the d-orbital. The values of β lies in the range of 0.59–0.72 indicating the appreciable covalent character of the metal–ligand bonding (Lever, 1984; Chandra et al., 2009; Dutta and Syamal, 1993).

3.5. ESR spectra

The ESR spectra of Cu(II) provide information about the extent of the delocalization of unpaired electron. The X-band ESR spectra of the Cu(II) complexes were recorded in the solid state at room temperature, their $g_{||}$, $g_\perp$, Δg, g_{av}, G have been calculated. The values of the ESR parameters $g_{||}$, $g_\perp$, g_{av}, Δg, G for Cu(II) complex of HL^1 are 2.2298, 2.1486, 2.1757, 0.0812, 1.5539, respectively. Similarly, the corresponding values for Cu(II) complex of HL^2 are 2.2564, 2.1831, 2.2075, 0.0733, 1.4054, respectively.

ESR spectra of the complexes revealed two g values ($g_{||}$ and $g_\perp$). Since the $g_{||}$ and $g_\perp$ values are closer to 2, $g_{||} > g_\perp$ suggests a tetragonal distortion around the Cu(II) ion. The trend $g_{||} > g_\perp > g_e(2.0023)$ shows that the unpaired electron is localized in $d_{x^2-y^2}$ orbital in the ground state of Cu(II), spectra are characteristic of axial symmetry. The $g_{||} > 2.3$ is a characteristic of an ionic environment and $g_{||} < 2.3$ indicates a covalent environment in the metal ligand bonding. The $g_{||}$ values for these complexes are less than 2.3 suggesting the environment is covalent. The exchange coupling interaction between two Cu(II) ions is explained by the Hathaway expression $G = (g_{||}-2.0023)/(g_\perp-2.0023)$. According to Hathaway, if the value G is greater than 4 ($G > 4.0$), the exchange interaction is negligible; whereas when the value of G is less than 4 ($G < 4.0$) a considerable exchange coupling is present in solid complex. The G values for these Cu(II) complexes are less than four indicating, considerable exchange interaction in the complexes (Hathaway and Billing, 1970; Mishra and Pandey, 2005).

3.6. Thermal analyses

The thermal behaviour of metal complexes shows that the hydrated complexes lose molecules of hydration first; followed by the decomposition of ligand molecules in the subsequent steps.

The thermal degradation behaviour of the Ni(II) complex of HL^1 has been studied by thermogravimetric analysis. The TGA curve of the complex shows no loss in weight up to 112 °C. Above this temperature a weight loss has been observed corresponding to two coordinated water molecules (remaining wt.%, obs./calcd., 94.60/93.98). After 225 °C, a weight loss has been observed in general up to 428 °C, indicating decomposition of the non-coordinated part of the ligand (remaining wt.%, obs./calcd., 46.3/41.84). The decomposition of the remaining ligand moiety occurs between 500 and 700 °C, above 700 °C a horizontal curve has been observed suggesting the ultimate pyrolysis product as metal oxide (remaining wt.%, obs./calcd., 23.25/21.78). The DTG curve of the complex shows peak at 150, 388, 636 °C (Mohamed et al., 2009).

The thermogram of the Co(II) complex of HL^2 shows that the complex is stable up to 105 °C. This indicates the absence of lattice water molecule in the complex. On increasing the temperature decomposition started between the temperature range of 105 and 200 °C, corresponding to the elimination of two coordinated water molecules (remaining wt.%, obs./calcd., 95.10/94.29). After this temperature, a loss in weight has been observed in general up to 340 °C corresponding to the loss of partially decomposed ligand part from the complex (remaining wt.%, obs./calcd., 64.32/62.61). Above 460 °C, a weight loss has occured up to 690 °C. This indicates the elimination of the remaining thermally degradable part of the complex. After 670 °C a horizontal curve has been observed which corresponds to a mixture of metal oxide as an ultimate pyrolysis product (remaining wt.%, obs./calcd., 24.45/21.40). DTG peak has been observed for the Co(II) complex at 174, 327, 643 °C (Al-Shihri and Abdel-Fattah, 2003).

The thermal analysis evaluating the thermal stability of the metal complexes, this study also helped to characterize the metal complexes.

3.7. Kinetic study

The kinetic evaluations of the thermal decomposition of the complexes were carried out. All stages were selected for the study of kinetics of decomposition of complexes. The kinetic parameters' data are summarized in Table 5. On the basis of thermal decomposition, the kinetic analysis parameter such as activation energy (E^*), pre-exponential factor (Z), entropy of activation (ΔS^*), enthalpy of activation (ΔH^*) and free energy of activation (ΔG^*) were calculated by using Piloyan and Novikova (1966) and Coats and Redfern (1964) equation:

$$\text{Piloyan} - \text{Novikova}: \quad \ln[\alpha/T^2] = \ln(ZR/\beta E^*) - E^*/RT$$

$$\text{Coats} - \text{Redfern}: \quad \ln[g(\alpha)/T^2] = \ln(ZR/\beta E^*) - E^*/RT$$

In the above equation, α is the fraction of the reacted material, T is the absolute temperature, $g(\alpha)$ is integral mechanism function, E^* is the activation energy in kJ/mol, Z is the pre-exponential factor, β is the heating rate and R is the gas constant. A straight line plot of the left hand side of the above equations against $1/T$ gives the value of E^* and Z from the

Table 5 Kinetic and thermodynamic parameters of complexes.

Complex	Method	Dec. stage/temp. (°C)	E^* (kJ mol^{-1})	Z (s^{-1})	ΔS^* (J K^{-1} mol^{-1})	ΔH^* (kJ mol^{-1})	ΔG^* (kJ mol^{-1})
[Ni(L^1)$_2$(H$_2$O)$_2$]	P-N	150/I	29.07	1.59×10^{-6}	-358.92	20.97	172.80
	C-R		40.56	3.68×10^{-2}	-275.30	32.46	148.92
	P-N	388/II	67.96	1.62×10^{-2}	-285.87	55.30	244.26
	C-R		90.33	1.18×10^{5}	-154.48	77.68	179.79
	P-N	636/III	72.87	1.19×10^{-6}	-367.67	55.468	389.67
	C-R		119.43	2.26×10^{3}	-190.01	102.03	274.74
[Co(L^2)$_2$(H$_2$O)$_2$]	P-N	174/I	33.12	4.51×10^{-5}	-331.54	24.57	172.76
	C-R		48.90	1.84×10^{1}	-224.10	40.34	140.51
	P-N	327/II	66.55	1.79	-245.92	55.06	202.61
	C-R		92.35	5.28×10^{8}	-83.77	80.86	131.12
	P-N	643/III	84.12	7.71×10^{-5}	-333.05	66.57	371.65
	C-R		120.18	1.46×10^{4}	-174.54	102.63	262.51

slope and the intercept, respectively. The entropy of activation (ΔS^*), enthalpy of activation (ΔH^*) and free energy of activation (ΔG^*) were calculated using the following equation:

$$\Delta S^* = 2.303(\log Zh/kT)\ R$$

$$\Delta H^* = E^* - RT$$

$$\Delta G^* = \Delta H^* - T\Delta S^*$$

where k and h are the Boltzmann and Planck constants, respectively.

The high values of the activation energies reflect the thermal stability of the complexes. The complexes have negative entropy, which indicates that the decomposition reactions proceed with a lower rate than the normal ones. The negative value of entropy also indicates that the activated complexes have a more ordered and more rigid structure than the reactants or intermediates. The negative values of the entropies of activation are compensated by the values of enthalpies of activation, leading to almost the same values for the free energy of activation (Wang et al., 2009; Mohamed et al., 2009).

3.8. X-ray diffraction study

X-ray diffraction was performed for metal complexes. The XRD patterns indicate crystalline nature for the complexes. X-ray powder diffractogram of the complexes were recorded using CuKα as the source in the range 5°–70° (2θ). X-ray crystal system has been worked out by trial and error methods for finding the best fit between observed, calculated Sin^2 θ. The diffractogram of Co(II) complex of HL^1 has recorded 17 reflections with maxima at 2θ = 21.38 with interplanar distance d = 4.15267. The complex is crystallized in the orthorhombic system. Sin^2 θ and hkl values for different lattice planes have been calculated. Crystal data for complex, a = 16.28824 Å, b = 22.25397 Å, c = 20.17538 Å, V = 7313.13 ^{3}, Z = 9, D_{obs} = 1.4043 g/cm^3, D_{cal} = 1.3554 g/cm^3. The Ni(II) complex of HL^2 has recorded 14 reflections with maxima at 2θ = 23.01 with interplanar distance d = 3.86205. The complex is crystallized in the tetragonal system. Sin^2 θ and hkl values for different lattice planes have been calculated. Crystal data for complex, $a = b$ = 15.07517 Å, c = 16.82242 Å, V = 3823.08 ^{3}, Z = 5, D_{obs} = 1.5011 g/cm^3, D_{cal} = 1.4852 g/cm^3. The observed and calculated values of density and Sin^2 θ show good agreement (Sujamol et al., 2010; Patange and Arbad, 2007).

3.9. Electrical conductivity

The temperature dependence of the solid state conductivity (σ) of the compounds in their compressed pellet form have been measured at fixed frequency 1 kHz in the temperature range 297–413 K. The values of the solid state electrical conductivity of the Schiff base and its complexes increase with increasing temperature, decrease upon cooling over the studied temperature range indicating its semi-conducting behaviour. The general behaviour of electrical conductivity follows the Arrhenius equation:

$$\sigma = \sigma_0 \exp(-E_a/KT)$$

where E_a is the thermal activation energy of conduction, σ_0 is the conductivity constant, K is the Boltzman constant. The lots of σ vs $1000/T$ for all the compounds are found to be linear over a studied temperature range. The electrical conductivity at room temperature are: Cr(III)-HL^1 = 1.21×10^{-6} ohm^{-1}cm^{-1}; Co(II)-HL^1 = 8.62×10^{-7} ohm^{-1}cm^{-1}; Ni(II)-HL^1 = 4.68×10^{-8} ohm^{-1}cm^{-1}; Cu(II)-HL^1 = 3.30×10^{-7} ohm^{-1}cm^{-1}; Cr(III)-HL^2 = 2.33×10^{-8} ohm^{-1}cm^{-1}; Co(II)-HL^2 = 7.12×10^{-8} ohm^{-1}cm^{-1}; Ni(II)-HL^2 = 5.42×10^{-10} ohm^{-1}cm^{-1}; Cu(II)-HL^2 = 6.26×10^{-9} ohm^{-1}cm^{-1}. These values show their semi-conducting nature. The electrical conductivity at room temperature for the complexes of HL^1 are Cr > Co > Cu > Ni and for the metal complexes of HL^2 are Co > Cr > Cu > Ni. The activation energy of the compound lies in the range 0.248–0.785 eV (Wahed et al., 2003; Makode et al., 2009). The confirmation of the temperature dependence conductivity of the compounds was also checked by repeating the conductivity measurements.

3.10. Antimicrobial activities

The in vitro Antimicrobial activity of the synthesized Schiff base ligands and their corresponding metal complexes on the selected bacteria E. coli and S. aureus and two fungi A. niger and C. albicans was carried out. All of the tested compounds showed good biological activity against microorganism. On comparing the biological activity of the Schiff base and its metal complexes with the standard bactericide and fungicide, it shows that some metal complexes have good activity as compared to the standard but all the complexes are more active than their respective ligands. The higher inhibition zone of

Table 6 Antibacterial screening data for the ligands and their complexes.

Compound	E. coli						S. aureus					
	Diameter of inhibition zone (mm)			% Activity index[a]			Diameter of inhibition zone (mm)			% Activity index[a]		
	25	50	100	25	50	100	25	50	100	25	50	100
HL^1	10	12	15	45	50	54	8	11	13	44	50	54
Cr(III)	12	14	17	55	58	61	11	14	19	61	64	79
Co(II)	17	20	25	77	83	89	15	19	21	83	86	88
Ni(II)	15	17	21	68	71	75	13	17	19	72	77	80
Cu(II)	17	20	24	77	83	86	14	18	20	78	82	83
HL^2	13	15	18	59	63	64	11	14	16	61	64	67
Cr(III)	15	17	20	68	71	71	13	16	18	72	73	75
Co(II)	18	22	26	82	92	93	15	19	21	83	86	88
Ni(II)	16	20	24	73	83	86	13	16	19	72	73	79
Cu(II)	17	20	25	77	83	89	16	20	22	89	91	92
Streptomycin (standard)	22	24	28	100	100	100	18	22	24	100	100	100

[a] $\%\text{Activity Index} = \dfrac{\text{Zone of inhibition by test compound(diameter)}}{\text{Zone of inhibition by standard(diameter)}} \times 100.$

Table 7 Antifungal screening data for the ligands and their complexes.

Compound	Diameter of inhibition zone (mm); concentration in ppm					
	A. niger			C. albicans		
	25	50	100	25	50	100
HL^1	13	16	21	12	16	21
Cr(III)	13	17	22	15	18	22
Co(II)	18	22	28	19	22	27
Ni(II)	15	19	24	17	19	24
Cu(II)	17	21	27	18	20	25
HL^2	10	12	16	12	14	17
Cr(III)	11	14	18	13	15	18
Co(II)	15	19	24	17	19	23
Ni(II)	15	18	23	16	19	22
Cu(II)	16	20	25	17	19	23
Miconazole (standard)	20	24	30	22	24	29

the metal complexes than those of the ligands can be explained on the basis of Overtone's concept and Chelation theory. On chelation, the polarity of the metal ion will be reduced to a greater extent due to the overlap of the ligand orbital and partial sharing of the positive charge of the metal ion with donor groups. Further, it increases the delocalization of the π-electrons over the whole chelating ring and enhances the penetration of the complexes into lipid membranes and blocking of the metal binding sites in the enzymes of microorganisms. There are other factors which also increase the activity are solubility, conductivity and bond length between the metal and ligand (Chohan et al., 2004, 2001; Tweedy, 1964).

The antibacterial data are listed in Table 6. The investigation of the antibacterial data revealed that the Co(II) and Cu(II) complex of HL^2 exhibited better antibacterial activity against E. coli and S. aureus compared to other compounds. The antifungal data of compounds are given in Table 7. The antifungal results show that the Co(II) complex of HL^1 displayed high activity against fungi in comparison to other compounds.

4. Conclusion

In the present research studies, our successful efforts are the synthesis of some new compounds from the conventional as well as microwave methods. These synthesized compounds are characterized by various physicochemical and spectral analyses. In the result of microwave-assisted synthesis, it has been observed that the reaction time decreased from hours to minutes and availability of the product within better yields compared to the classical method. The synthesized Schiff base ligands bind with the metal ions in a bidentate manner, with ON donor sites of the deprotonated phenolic-O and azomethine-N. The ^{1}H-NMR data suggest that both the Schiff base ligands deprotonated after complexation. FAB-mass and thermal data show degradation pattern of the complexes. Thermogravimetric study of the complexes also helped to characterize these complexes. The XRD patterns indicate crystalline nature of the complexes. Electrical conductivity data suggest that all the complexes fall in the semi-conducting range. The antimicrobial data show the metal complexes to be more biologically

active compared to those parent Schiff base ligands against all pathogenic species. The compounds also inhibit the growth of fungi and bacteria to a greater extent as the concentration is increased.

Acknowledgements

References

Abdallah, S.M., Zyed, M.A., Mohamed, G.G., 2010. Arabian J. Chem. 3, 103.

Al-Shihri, A.S.M., Abdel-Fattah, H.M., 2003. J. Therm. Anal. Cal. 71, 643.

Chandra, S., Kumar, U., 2005. Spectrochim. Acta 61A, 219.

Chandra, S., Jain, D., Sharma, A.K., Sharma, P., 2009. Molecules 14, 174.

Chohan, Z.H., 1999. Met. Based Drugs 6, 75.

Chohan, Z.H., Munawar, A., Supuran, C.T., 2001. Met. Based Drugs 8, 137.

Chohan, Z.H., Pervez, H., Rauf, A., Khan, K.M., Supuran, C.T., 2004. J. Enzyme Inhib. Med. Chem. 39, 417.

Coats, A.W., Redfern, J.P., 1964. Nature 201, 68.

Dubey, R.K., Dubey, U.K., Mishra, C.M., 2008. Indian J. Chem. 47A, 1208.

Dutta, R.L., Syamal, A., 1993. Elements of Magneto Chemistry, second ed. Affiliated East West Press, New Delhi.

Garg, R., Saini, M.K., Fahmi, N., Singh, R.V., 2006. Trans. Met. Chem. 31, 362.

Hathaway, B.J., Billing, D.E., 1970. Coord. Chem. Rev. 5, 143.

Issa, R.M., Khedr, A.M., Rizk, H., 2008. J. Chin. Chem. Soc. 55, 875.

Lever, A.B.P., 1984. Inorganic Electronic Spectroscopy, second ed. Elsevier, New York.

Mahajan, K., Fahmi, N., Singh, R.V., 2007. Indian J. Chem. 46A, 1221.

Mahajan, K., Swami, M., Singh, R.V., 2009. Russ. J. Coord. Chem. 35, 179.

Makode, J.T., Yaul, A.R., Bhadange, S.G., Aswar, A.S., 2009. Russ. J. Inorg. Chem. 54, 1372.

Mishra, A.P., Pandey, L.R., 2005. Indian J. Chem. 44A, 94.

Mishra, A.P., Soni, M., 2008. Met. Based Drug 1. doi:10.1155/2008/875410.

Mishra, A.P., Mishra, R.K., Shrivastava, S.P., 2009. J. Serb. Chem. Soc. 74, 523.

Mohamed, G.G., Omar, M.M., Ibrahim, A.A., 2009. Eur. J. Med. Chem. 44, 4801.

Mohanan, K., Kumari, B.S., Rijulal, G., 2008. J. Rare Earths 26, 16.

Nakamoto, K., 1998. Infrared and Raman Spectra of Inorganic and Coordination Compounds, Part A & B, fifth ed. John Wiley & Sons, New York.

Neelakantan, M.A., Marriappan, S.S., Dharmaraja, J., Jeyakumar, T., Muthukumaran, K., 2008. Spectrochim. Acta 71A, 628.

Omar, M.M., Mohamed, G.G., 2005. Spectrochim. Acta 61A, 929.

Ourari, A., Ourari, K., Moumeni, W., Sibous, L., 2006. Trans. Met. Chem. 31, 169.

Patange, V.N., Arbad, B.R., 2007. J. Indian Chem. Soc. 84, 1096.

Piloyan, G.O., Novikova, O.S., 1966. Russ. J. Inorg. Chem. 12, 313.

Raman, N., Raja, S.J., Joseph, J., Raja, J.D., 2007. J. Chil. Chem. Soc. 52, 1138.

Sharma, K., Singh, R., Fahmi, N., Singh, R.V., 2010. Spectrochim. Acta 75A, 422.

Soliman, A.A., Mohamed, G.G., 2004. Thermochim. Acta 421, 151.

Spinu, C., Kriza, A., Spinu, L., 2001. Acta Chim. Slov. 48, 257.

Sujamol, M.S., Athira, C.J., Sindhu, Y., Mohanan, K., 2010. Spectrochim. Acta 75A, 106.

Sun, Y., Machala, M.L., Castellano, F.N., 2010. Inorg. Chim. Acta 363, 283.

Tweedy, B.G., 1964. Phytopathology 55, 910.

Wahed, M.G., Bayoumi, H.A., Mohamme, M.I., 2003. Bull. Korean Chem. Soc. 24, 1313.

Wang, Y.F., Liu, J.F., Xian, H.D., Zhao, G.L., 2009. Molecules 14, 2582.